ISSN 0027-1349, Moscow University Physics Bulletin, 2015, Vol. 70, No. 4, pp. 282–290. © Allerton Press, Inc., 2015.
Original Russian Text © E.A. Bruevich, G.V. Yakunina, 2015, published in Vestnik Moskovskogo Universiteta. Fizika, 2015, No. 4, pp. 66–74.

ASTRONOMY, ASTROPHYSICS, AND COSMOLOGY

The Cyclic Activity of the Sun from Observations of the Activity Indices at Different Time Scales

E. A. Bruevich and G. V. Yakunina

Sternberg Astronomical Institute, Moscow State University, Universitetskii pr. 13, Moscow, 119991 Russia
e-mail: red-field@yandex.ru; yakunina@sai.msu.ru

Received April 3, 2015; in final form, April 29, 2015

Abstract—With the time–frequency analysis of the series of observations of one of the global indices of solar activity, viz., the radio flux $F_{10.7}$ at a wavelength of 10.7 cm (2.8 GHz), the most probable value of the main cycle period has been determined. This value is 10.2 yr, which is consistent with the generally accepted estimates. Simultaneously with the main cycle of activity, several low-amplitude cycles with cyclicity periods from 1.3 to 100 yr were identified. With the method of continuous wavelet transform with Morlet mother wavelets, we analyzed the other solar indices that are associated with the radiation at different heights in the solar atmosphere: the relative number of sunspots, SSN, the chromospheric index, *Mg II*, at 280 nm, the fluxes in the coronal line at 530.3 nm, F_{530}, the *Flare Index*, and the index of a total number of flares, *Counts of flares*. The obtained time–frequency characteristics turned out to be generally similar. Differences in the results for the solar indices occur during the strengthening of stochastic processes in the maxima and minima of the main cycle.

Keywords: solar activity, activity indices, solar activity cycles.

DOI: 10.3103/S0027134915040062

INTRODUCTION

Solar activity is basically a complex of the phenomena and processes that are connected with the evolution of magnetic fields in the solar atmosphere. The study of solar activity is of high fundamental and practical importance for the forecasting of the cosmic climate and the processes in the terrestrial atmosphere. Since 1749 the solar activity has been estimated by the index of the relative number of sunspots or the Wolf number (SSN).

The variability of the radio emissions of the Sun was detected at ground-based observatories in the 20th century. Regular radio observations of the emission variability of the chromosphere and lower corona began in 1947; they initiated the studies of a new global index, viz., the radio flux at a wavelength of 10.7 cm (2.8 GHz), $F_{10.7}$. This index is directly connected with the radiation from the entire disk; this is currently used in the monitoring and forecasting of the solar activity more frequently than the other quantities are. The variability of the solar radio emissions is also characterized by cyclicity; the length of radio cycles is the same as that of the main 11-year cycle of the spot-producing activity of the Sun (the Schwabe–Wolf cycle). The most important characteristic of a sunspot is its magnetic field. The change in the number of sunspots means that the complex of local magnetic fields on the Sun changes. The full solar cycle (the Hale cycle) is connected with the evolution of both the local fields and the global magnetic field of the Sun; it is equal to two 11-year cycles.

At present, the cyclical variability of the solar radiation is considered as a consequence of the cyclic changes of the magnetic field of the Sun. During the Schwabe–Wolf cycle, the complex evolution of magnetic fields takes place: the magnetic lines reconnect with each other and the magnetic energy is transformed into the kinetic and thermal energy of plasma fluxes. In total, the magnetodynamic processes lead to the formation of active zones in the atmosphere of the Sun: flares and spots in the photosphere, floccules in the chromosphere, and prominences in the corona. This problem is also of fundamental importance for the astrophysics of stars rather than only of the Sun. Its applied significance is connected with the influence of the active solar processes on the magnetic field of the Earth. While our understanding of the physics of active zones is still not complete, we cannot forecast the details of the evolution of each of the zones. However, we may diagnose the collective dynamics of active zones by studying the cyclic variability of the solar radiation that is induced by the energy release in the active zones. This variability actually allows us to analyze the physical processes that occur, not only in the solar atmosphere, but also in the layers under the photosphere [1]. In addition, from the data on the cyclic variability, the amplitude of the magnetic activity cycle of the Sun can be predicted, which is of key importance for studying processes in the atmosphere of the Earth.

At the present time, in order to survey the situation on the Sun and make different prognoses, several global indices of the solar activity are continuously monitored. We examined these indices and their mutual correlation for solar cycles 21, 22, and 23 [2]. The high degree of correlation between the flux at a wavelength of 10.7 cm and all of the main indices of activity suggests that there is a strong dependence of the indices on the parameters of the plasma, where these fluxes are formed, while the regions of their formation are close in space. We may also note that $F_{10.7}$ is closely related to the X-ray fluxes from the entire solar disk. When the activity is high, these fluxes correlate with each other well. However, when the activity is low and the X-ray flux is insufficient for detection, the correlation becomes weak [3]. Our analysis of the correlation relationships between $F_{10.7}$ and the X-ray fluxes for different levels of the solar activity [2] confirms the conclusions of [3].

The monitoring of $F_{10.7}$ is also a useful tool for predicting the variations of the solar coronal EUV (extreme ultraviolet) radiation, which changes by an order of magnitude in dependence on the amount and brightness of the solar active zones. Exactly the fluxes in the EUV range play a key role in the heating of the terrestrial thermosphere and, consequently, in the formation of the Earth's climate. Since the total flux, $F_{10.7}$, correlates rather well with the integrated fluxes in the UV and EUV ranges of the solar spectrum, it can be used as a basic index for forecasting the fluxes in these intervals of the solar spectrum as well [4, 5]. The radio flux at a wavelength of 10.7 cm from the entire solar disk can be divided into three components (in terms of the characteristic time scales): (i) events that last less than 1 hour that are associated with the flare activity; (ii) slow variations of intensity that last from several hours to several years and are connected with the evolution of active zones (in the cyclic activity of the Sun, it is designated as S-component); and (iii) the so-called "quiet Sun level," when the intensity never drops lower than the minimum level of the flux $F_{10.7}$ [6]. According to the observations, there is a close correlation between the S-component of the radio emission at 10.7 cm and the fluxes in the Ca II and Mg II lines. The flux at a wavelength of 10.7 cm increases with an increase in the temperature, material density, and magnetic fields, which makes it a sensitive indicator of the general level of the solar activity. In the present paper we use the NASA archives of the observational data on the solar-activity indices [7].

The purpose of the present paper is to study the evolution of the solar cyclicity since 1950 to 2014 from the observations of the global indices of activity that are formed at different levels in the solar atmosphere. The time series of observations were considered with the wavelet-analysis using the Morlet wavelet as the most suitable one for astronomic data. Along with the main activity cycle that has the maximum amplitude, the cyclicities with substantially lower amplitudes are also investigated.

1. A TIME–FREQUENCY ANALYSIS OF A SERIES OF OBSERVATIONS OF THE SOLAR ACTIVITY INDICES

The wavelet transform of signals is a result of developing the methods of spectral analysis, whose typical representative is the classic Fourier transform. The term "wavelet" originates from an English word for a small (short) wave. Wavelet is a generic name for families of mathematical functions of a specific form. These families are local in time and frequency; all their functions are generated from the basic (mother) one by shifts and extensions in time.

As distinct from spectral analysis, the wavelet transform yields a two-dimensional evolvent of the considered signal; the time and frequency are independent variables. Such a representation allows the properties of the signal to be simultaneously investigated in the time and frequency domains. Wavelet analysis is a perfect tool for considering the signals with frequency characteristics that are variable in time. It should not be supposed that wavelet analysis takes the place of the classic Fourier analysis. They supplement each other and can be effectively used together. The Fourier transform yields the complete information on the spectral characteristics of the signal in the considered frequency range, while the variations of these characteristics in time can be studied using wavelet analysis.

To analyze a signal or an image, the mother wavelet should be chosen in accordance with the considered problem or the character of the studied signal. The main application area of wavelet transforms is the analysis and processing of signals and functions that are nonstationary in time or nonuniform in space. In these cases, the results of the analysis should contain not only the frequency characteristic of the signal (the energy distribution through the frequency components), but also the information on the local coordinates, where some groups of frequency components manifest themselves or quick variations of the frequency components of the signal occur. In [8, 9] it was shown that the modern methods of spectral analysis, specifically, wavelet analysis, allow the data of observations of the solar activity on different time scales to be successfully processed. Thus, wavelet analysis has an advantage over the Fourier transform, because the latter yields only the information on the set of periods, but does not determine where the change of the period occurs [10]. The continuous wavelet transform of the function $s(t)$ is a function of two variables

$$C(a, b) = \langle s(t)\psi(a, b, t)\rangle,$$

where the wavelets $\psi(a, b, t) = C_{(a,b)}(t)$ are the scaled and shifted versions of the mother wavelet $\psi(t)$.

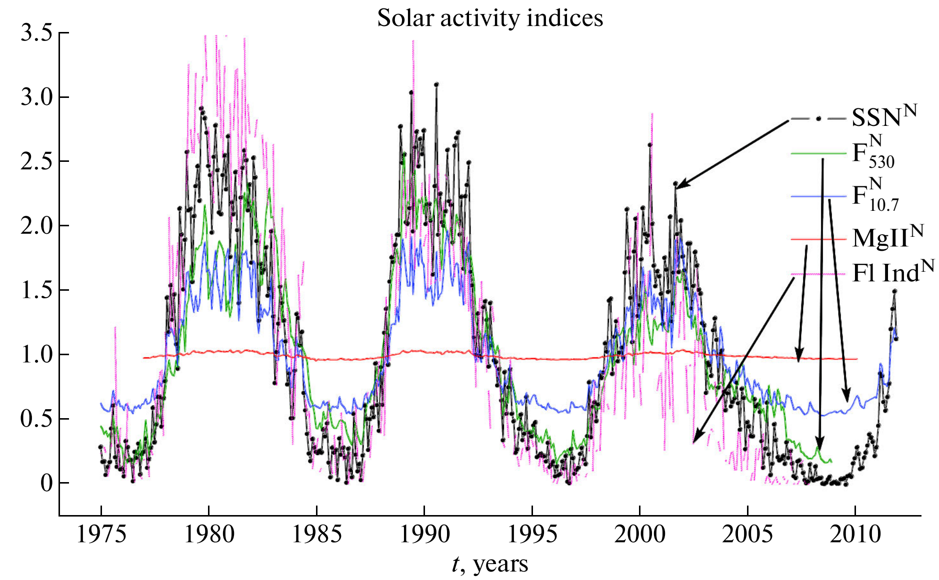

Fig. 1. The time series of observations of the solar activity indices: SSN, the $F_{10.7}$ and F_{530} fluxes at wavelengths of 10.7 cm and 530.3 nm, respectively, *Mg II* at 280 nm, and *Flare Index*. The superscript *N* means that the observational data were normalized to their mean values (calculated for the time of observation).

Thus, in the function of two independent variables (a, b), the arguments a and b vary in units of frequency and time, respectively:

$$\psi_{ab}(t) = (1/\sqrt{|a|})\psi((t-b)/a),$$

$$C(a, b) = (1/\sqrt{|a|})\int_{-\infty}^{\infty} s(t)\psi((t-b)/a)dt.$$

We analyzed the observations of the main indices of solar activity for the last three cycles. The relative amplitudes of variations of these indices are displayed in Fig. 1. It is seen that different indices demonstrate strongly differing relative amplitudes of variations: from fractions of a percent to 3.5 times. The activity indices describing the X-ray emission of the Sun, which are not considered here, may vary even more strongly in the activity cycle, viz., by 2–3 orders of magnitude.

The most widely used method of presentation of wavelet-analysis results is the projections of the wavelet spectrum coefficients $C(a, b)$ on the time-frequency plane (a, b) with curves that show constant levels, which makes it possible to trace the changes of the coefficients at different time scales and to reveal the pattern of the local extrema of these projections. The wavelet portrait of the observational series of SSN as a projection of the wavelet spectrum coefficients $C(a, b)$ on the time-frequency plane is shown in Fig. 2.

From the energy density $E(a, b) = C^2(a, b)$, the local energy density can be determined for the specified time and frequency, and the temporal dynamics of the redistribution of energy through the scales, i.e., the energy exchange between the components of different scales at any specified point of time, can be analyzed. In Fig. 3 we show the three-dimensional wavelet portrait on the same SSN series as that in Fig. 2. The *xy* plane corresponds to the frequency–time plane (a, b): a is along the y axis (periodicity, years), b is along the x axis (time, years), and the z axis presents the dynamics $C^2(a, b)$ (the energy density). The temporal dynamics of the redistribution of energy of the process through the scales suggests that the maximum energy is concentrated at the frequencies that correspond to the 11- and 22-year solar cycles. Choosing the wavelet that is used in the time–frequency decomposition is the most important task. This choice influences the resolution of the result by time and frequency. We cannot change the main characteristics of the wavelet transform (the low frequencies show a high resolution in frequency and a low resolution in time, while the high frequencies show a low resolution in frequency and a high resolution in time), but we may somewhat increase the total resolution in frequency or time. When we use the Morlet wavelet (its real part is a damped function of the cosine), we obtain a high resolution in frequency, which is important for the processing of astronomical observations [9, 10].

2. THE GLOBAL INDICES OF SOLAR ACTIVITY ON DIFFERENT TIME SCALES: RESULTS OF THE ANALYSIS OF THE OBSERVATIONAL SERIES

As discussed above, the index of radio emission of the Sun at a wavelength of 10. 7 cm was chosen for the analysis of the temporal evolution of the solar cyclicity,

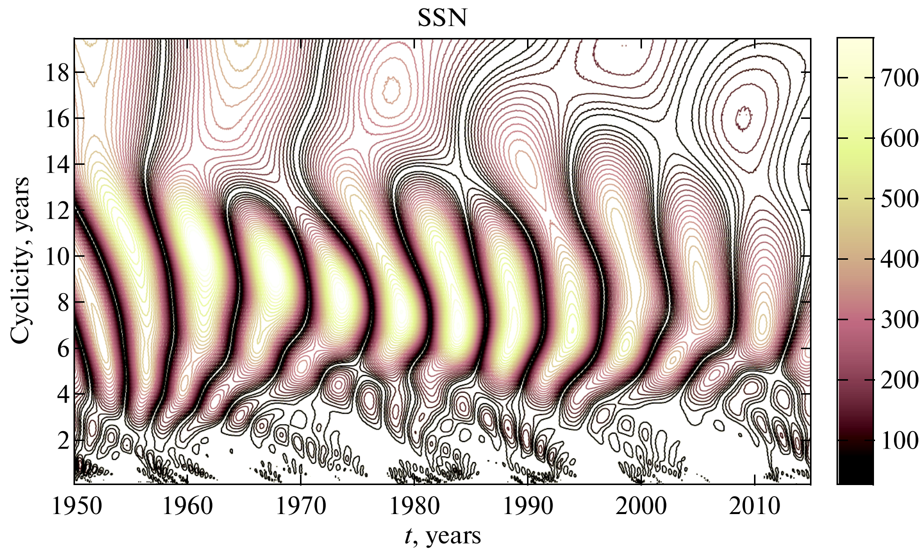

Fig. 2. The wavelet portrait of the series of observations of SSN as a projection of the wavelet coefficients $C(a, b)$ on the frequency–time plane (a, b) with the curves of constant levels.

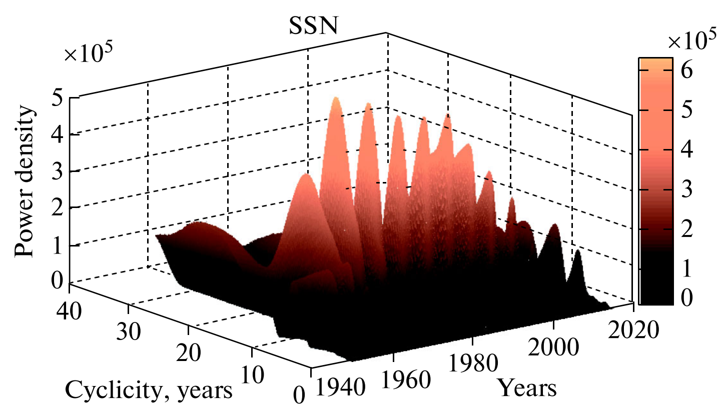

Fig. 3. The three-dimensional wavelet portrait of the series of observations of SSN using the Morlet mother real-valued wavelet.

because this parameter is generally accepted as the most objective index of the global solar activity; moreover, it is closely related to the radiation fluxes from the entire solar disk in different spectral ranges. In [8, 9] the authors analyzed the potential of different mother wavelets that are used in astronomical applications, particularly, in studying the series of observations of the solar activity indices and the radiation of one quasar. It was concluded that the most appropriate method for processing astronomical observations is the Morlet wavelet, which in addition is maximally close to the classic Fourier transform for each of the individual points on the time axis. We compared the time series of the solar activity index $F_{10.7}$ with different mother wavelets: Daubechies 10, Symlet 8, Meyer, Gauss 8, and real- and complex-valued Morlet wavelets [11].

The Morlet mother wavelet combines the characteristics of the plane wave and the Gaussian function:

$$\psi(t) = e^{-t^2/a^2} e^{2i\pi t}.$$

The combination of these two functions in one mother wavelet allows one to successfully investigate the characteristics of temporal variations of astronomical signals from the Sun, quasars, and other objects that contain an expressed cyclic component. In the study of the variations of the fluxes from the Sun, the processing of observations with the Mortel wavelet yielded the most successful results.

In Fig. 4 the results of the wavelet analysis of the time series of the monthly average values of $F_{10.7}$ are presented; the time and cyclicity (both in years) are along the x and y axes, respectively. The set of coefficients of the function $C(a, b)$ characterizes the proba-

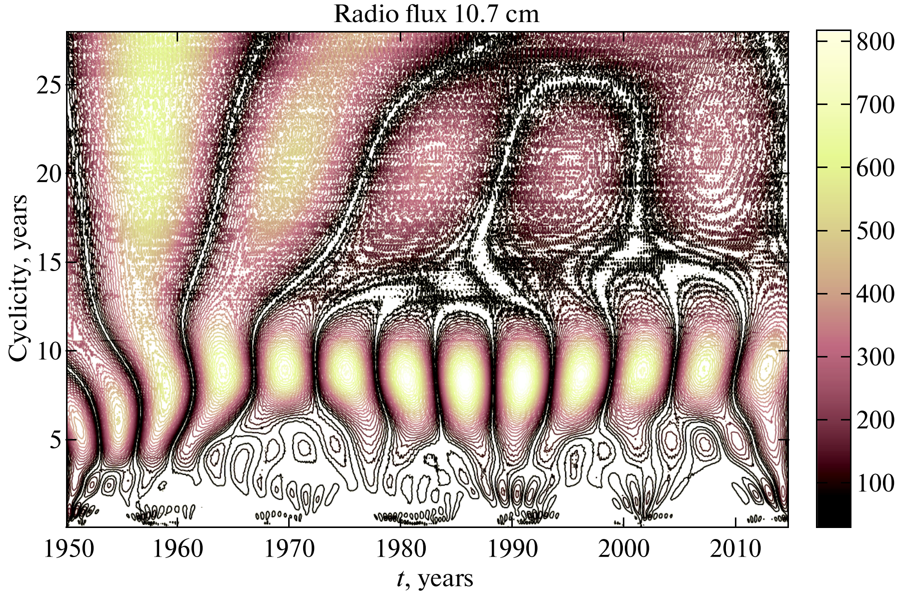

Fig. 4. The wavelet portrait of the series of the monthly average values of $F_{10.7}$.

bility amplitude for localization of exactly the regular cyclic component of the signal at the point (a, b). Since the Morlet wavelet portrait is very compact in frequency, the localization of the instantaneous frequency of the observed signal can be determined most accurately (as compared to the use of the other wavelets). As in the case of the SSN analysis (Fig. 2), the main cycle of activity is estimated with the best confidence; the most probable value of the periods of this cyclicity is approximately 10 years for $F_{10.7}$. In Fig. 4, within each of the 11-year cycles, we also see several quasi-biennial cycles, whose length decreases from 3 years at the beginning of the main cycle to 2.5 years at the end, which confirms the conclusions of [12]. We note that the phenomenon of cyclic periodicity of the radiation fluxes is also characteristic of the solar-type stars of the spectral classes G and K. These stars demonstrate clearly distinguishable cycles of activity that are analogous to the 11-year and quasi-biennial cycles. Moreover, for these stars, as for the Sun, a close relationship between the radiation fluxes from photospheres and the soft X-ray radiation has been revealed [13].

From the analysis of the time series of $F_{10.7}$ with the Morlet complex-valued wavelet applied to the anomalously long cycle 23, the peculiarities of the evolution of the main 11-year cycle of activity were revealed. According to the observations of the local magnetic fields and SSN, the length of cycle 23 is approximately 12.2 years. However, analysis with other wavelets failed to confirm this. With the Morlet complex-valued wavelet, we now obtain the dependence on two parameters: f_b, determining the width of the wavelet filter, and f_c, specifying the local center of the wavelet frequency. The basic function of the Morlet complex-valued wavelet is defined as follows:

$$\psi(x) = \frac{1}{\sqrt{\pi f_b}} e^{2i\pi f_c x} e^{-x^2/f_b}.$$

Figure 5 shows the analysis of the time series of the monthly average values of $F_{10.7}$ with the Morlet complex-valued wavelet. In this case, two additional parameters are varied in accordance with the problems that are to be solved. In an analogous manner to Fourier analysis, we obtain an array of the coefficients that describe not only the time-frequency distribution of the amplitude, but also the time-frequency distribution of the phase of the signal. It was found that the parameters of the Morlet complex-valued mother wavelet of 1.5-1 describe the evolution of the 11-year cycle best of all, because the less expressed and irregular cycles (quasi-biennial cycles and those with shorter periods) are suppressed. We also see that the period of activity cycle 23 is approximately 12 years, which agrees with the observations of the magnetic fields and sunspots.

Thus, the wavelet representation of the time series of the $F_{10.7}$ index allows us to analyze the temporal evolution of the periods of the main and supplementary activity cycles, rather than only to reveal them. Our analysis of the solar-activity cyclicity showed that the Morlet mother wavelet is the most appropriate one for studying the solar cyclicity [11]. The cycles with smaller amplitudes can be analyzed with the wavelets defined in such a way that the main cyclicity is suppressed.

To reveal the cyclicity on the 5-year and quasi-biennial time scales, we used the series of the monthly average values of the relative number of sunspots (the

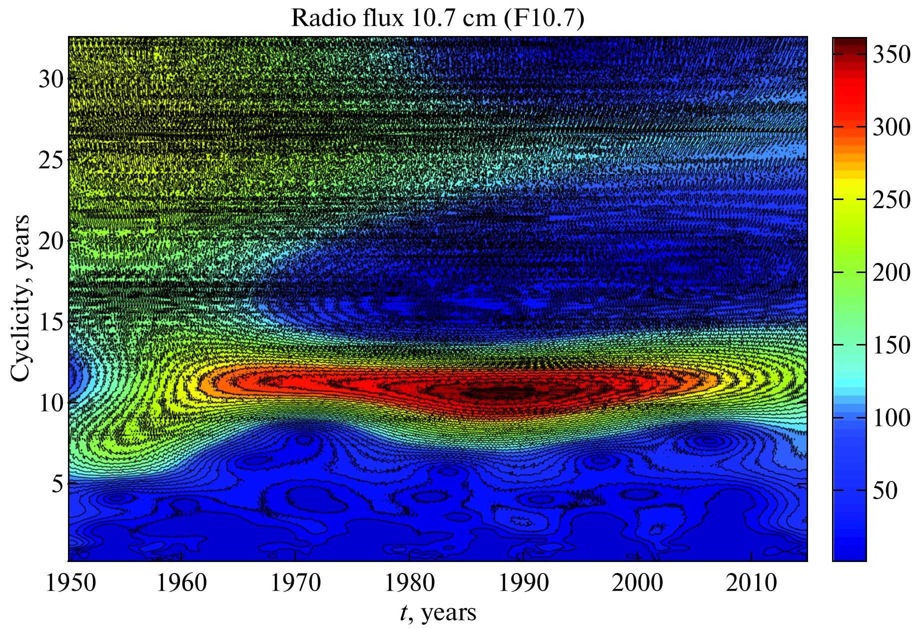

Fig. 5. Analysis of the time series of $F_{10.7}$ using the Morlet mother real-valued wavelet of 1.5–1.

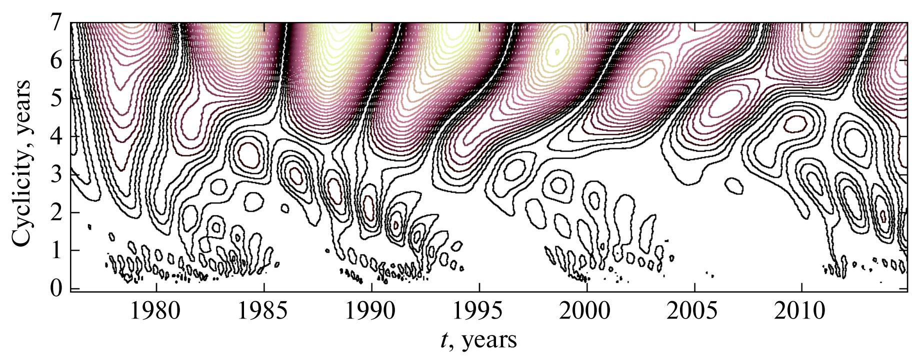

Fig. 6. The wavelet portrait of the time series of SSN on a scale of the cycle period less than 6 years. The Morlet real-valued wavelet is used.

data of the SSN observations for 1950–2014). These data were analyzed with the Morlet wavelet on a shorter time scale (Fig. 6). Cycles with 5.5-year, quasi-biennial, and annual periods can be noted. The existence of a 1.3-year cyclicity was also mentioned in [14]. Previously, during the recent decades, cyclicities with 5.5-year and quasi-biennial periods have been observed in the index of sunspots. It is difficult to study these cyclicities, because the amplitudes of their variations are much lower than those of the main 11-year cycle. Moreover, the periods of these low-amplitude cycles substantially changed during the main cycle. For example, it was observed that the periods of quasi-biennial cycles decreased from 3.5 to 2 years several times during the main 11-year cycle [15]. The instability of the periods of the cycles with smaller amplitudes did not allow the solar data to be analyzed with the Fourier transform. The wavelet analysis method is suitable for studying such actively evolving cycles.

Since the behavior of the solar activity in the past [8, 16, 17] attracts the attention of researchers, we believe that it is important to analyze the series of the solar observations at the century and longer time scales. Figure 7 presents the wavelet analysis of a series of the average annual values of SSN (from 1700 to 2014) on the scale of the cycle periods of less than 150 years using the Morlet real-valued wavelet. Besides the main 11-year cycle, we see cycles that are half a century and a century long and their evolution in time. For the period from 1700 to 1850, the relative number of sunspots was obtained from so-called proxies, viz., the indirect data from observations of solar activity. From 1850 until the present, direct observations of the relative number of sunspots have been car-

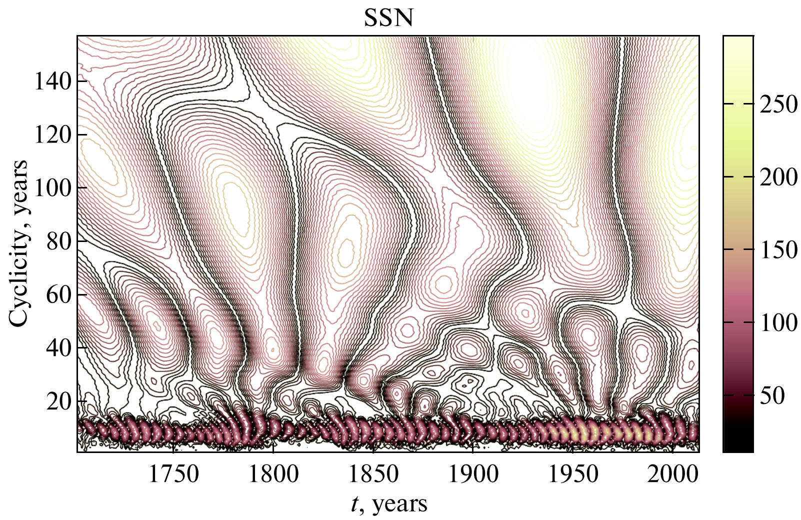

Fig. 7. The time–frequency analysis of the relative number of sunspots. The wavelet portrait of the time series of the average annual values of SSN on a scale of the cycle period of less than 150 years.

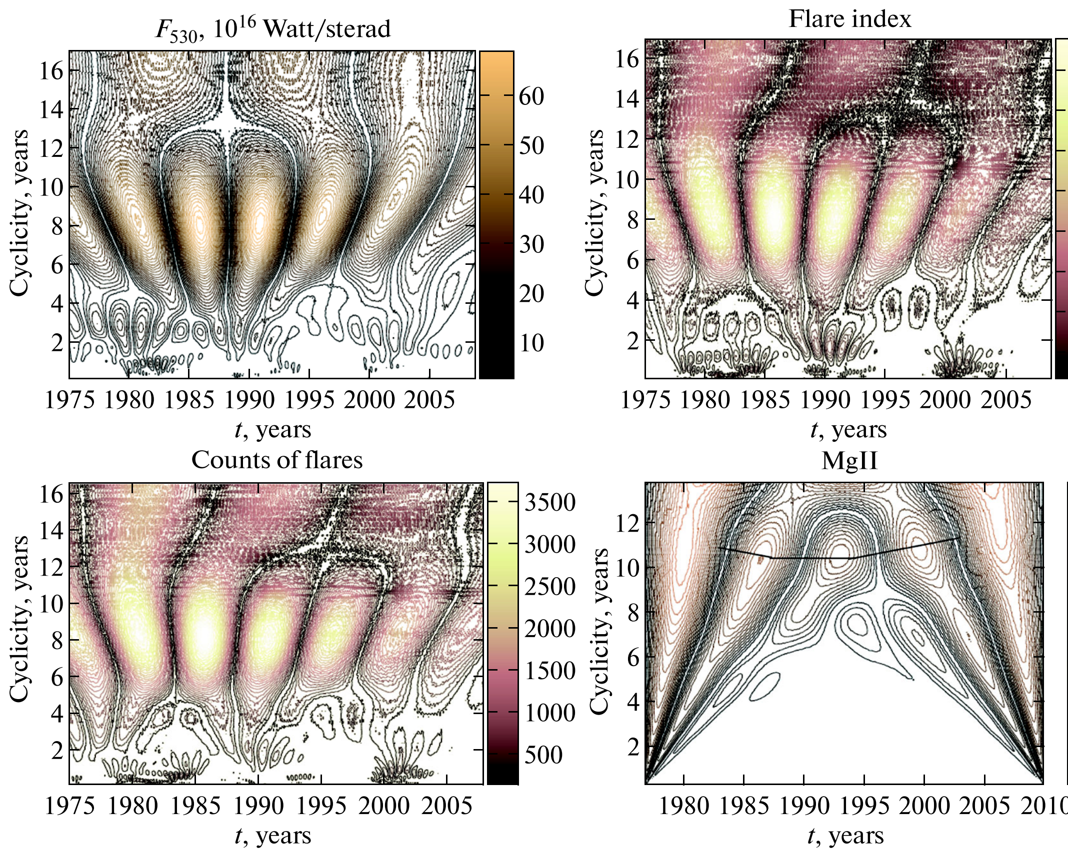

Fig. 8. The time–frequency analysis of the solar activity indices: F_{530}, *Flare Index*, *Counts of flares*, and *Mg II* at 280 nm. The wavelet portraits (the Morlet real-valued wavelet) are presented as projections of the wavelet coefficients $C(a, b)$ on the frequency–time plane (a, b) with the curves of constant levels.

ried out; starting from 1950 the radio emission fluxes at a wavelength of 10.7 cm and the other global solar indices have been directly determined.

In Fig. 8 the following solar activity indices that were studied with the wavelet analysis are presented: the *Flare Index*, *Counts of flares*, the fluxes in the coronal line of 530.3 nm, and the chromospheric index *Mg II* at 280 nm. Figure 8 shows the wavelet portraits of the series of observations of the activity indices that were obtained with the Morlet real-valued wavelet.

This allows us to compare the wavelet portraits of the activity indices that characterize the radiation fluxes that formed at different heights in the solar atmosphere. For all of the indices, the temporal evolution of both the main 11-year cycle and the cycles with the 5.5-year and quasi-biennial periods can be traced. The exception is the analysis of the flux in the chromospheric line *Mg II* at 280 nm, where we may see only the 11-year cycle. This is connected with the very low relative amplitudes of oscillations in the activity cycle for the *Mg II* index; they amount to approximately 0.1–0.2%. One should also take the fact into account that the observational data that are obtained with different instruments onboard several satellites have to be reduced to a single standard, which increases the weight of the relative error. As a result, it turned out that the time–frequency analysis of the series of observations of the chromospheric index *Mg II* cannot be reliably performed. This fact is an indirect limitation of the applicability of the method: if the signal-to-noise ratio is lower than the threshold quantity that is determined in each particular case by practical consideration, the application of the wavelet analysis method yields no reliable results.

The wavelet analysis method allows one to determine the most probable values of the dominating frequencies (if they exist) in the observational series and to trace their evolution in time. Simultaneously, the question of the accuracy of determining the most probable values of the required dominating frequencies arises. We indirectly estimated the accuracy of determining the probability of the maximum value for the dominating frequency as compared to the other frequencies at a specified point of time. In our case the probability is defined by the value of the wavelet coefficient $C(a, b)$ calculated for a specified point of time (a and b correspond to the periodicity and the time, respectively, both measured in years).

Figure 9 shows the sections (local portraits) of the wavelet coefficients $C(a, b)$ for fixed points in time. The Morlet real-valued wavelet for the series of observations of SSN (see Fig. 2) was used. Three dates of observations of the SSN index in solar cycle 23 were analyzed: in the activity minimum in mid 1996, in the phase of growth in mid 1998, and in the activity maximum in mid 2001. The shape of the curves that describe the array section of the wavelet coefficients $C(a, b)$ is similar to that for the normal distribution of deviations from the average. This property of the local portraits of the wavelet coefficients $C(a, b)$ is determined by the Morlet mother wavelet, which combines the characteristics of a plane wave and the Gaussian function. Thus, at the half-width level of the curve in Fig. 8, we may estimate the accuracy of determining the cycle period; this estimate corresponds to the root-mean-square deviation of the normal distribution and equals 1σ.

It is seen that the wavelet portrait for the phase of growth, viz., the middle of the cycle (1998), exactly

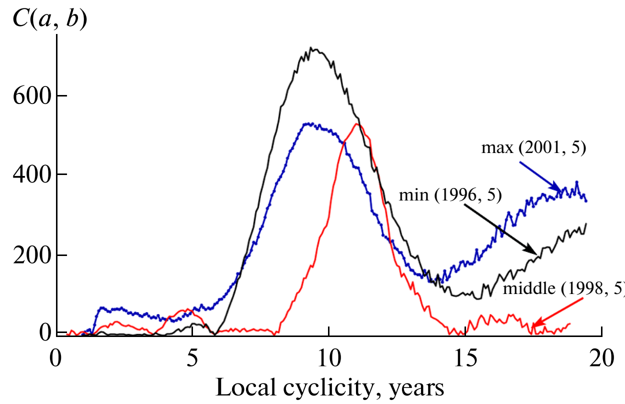

Fig. 9. Sections of the array of the wavelet coefficients, $C(a, b)$, for the series of observations of SSN for three observation dates of solar cycle 23 fixed at the phase of the minimum (1996.5), the phase of growth (1998.5), and the phase of the maximum (2001.5).

corresponds to a 10–11-year cycle. In addition, the root-mean-square deviation is minimum in this case: $1\sigma \sim 1$ year. At the minimum and maximum of the cycle (1996 and 2001; see Fig. 8), the extrema of the local wavelet portraits correspond to the period of the main cycle that is shorter than 10 years. The analysis of the sections of the wavelet coefficients $C(a, b)$ for a fixed point of time, the second maximum at the beginning of 2001, showed that three periodicities from 6 to 14 years long are actually distinguished in the local wavelet portrait of the main period. This confirms the influence of the stochastic processes on the regular local cyclicity at the moments of maxima and minima of the cycles. Moreover, the scattering of the wavelet coefficients around the mean value substantially increases in the minimum and maximum of the cycle (the root-mean-square deviation $1\sigma \sim 1.5$ year) as compared to that in the center, which is consistent with the conclusions of [2]. In the middle of the cycle, one may clearly observe a local maxima with a smaller amplitude on the 5.5-year and quasi-biennial scales. Thus, from the calculations of the wavelet coefficients $C(a, b)$ for the phases of the growth and decline of the main cycle beyond the minima and maxima, we obtain the values of the cycle period of 10–10.5 years that are determined from observations in the 20th century.

CONCLUSIONS

(1) For all of the considered activity indices, the length of the main cycle coincides with that of the Schwabe–Wolf cycle (see Figs. 2, 4, 5, 7, and 8). Along with this main cycle of activity that is at it maximum amplitude, wavelet analysis allows the periodicities of a substantially lower amplitude to be revealed. We confirmed the existence of 5.5-year and quasi-biennial cyclicities not only for the sunspot index, but also for $F_{10.7}$ and F_{530}, *Flare Index*, and *Counts of flares*. For all

of the activity indices, the results of the wavelet transform are generally rather similar; however, some differences are observed, especially at the maxima and minima of the 11-year cycles.

(2) The study of the cyclicity evolution of $F_{10.7}$ with the Morlet and Gauss wavelets yields results that agree better with the observations than those using other mother wavelets, such as the Meyer, Daubechies, and Symlet wavelets.

(3) The time-frequency analysis of the observational series of solar activity that was performed with different mother wavelets shows that the mean length of the Schwabe–Wolf cycle was approximately 10.2 years for all of the 20th century. For the activity cycle 23, the analysis of the observational series of $F_{10.7}$ with the Morlet complex-valued wavelet yields the actually observed value of 12.5 years for the length of the anomalous cycle 23.

REFERENCES

1. I. Rozgacheva and E. Bruevich, Astron. Astrophys. Trans. **21**, 27 (2002).
2. E. Bruevich, V. Bruevich, and G. Yakunina, J. Astrophys. Astron. **35**, 1 (2014).
3. A. Kruger, *Introduction to Solar Radio Astronomy and Radio Physics* (Springer, Dordrecht, 1979).
4. R. F. Donnelly, D. F. Heath, J. L. Lean, and G. J. Rottman, J. Geophys. Res. **88**, 9883 (1983).
5. R. D. Chapman and W. M. Neupert, J. Geophys. Res. **79**, 4138 (1974).
6. K. F. Tapping and B. de Tracey, Sol. Phys. **127**, 321 (1990).
7. http://www.ngdc.noaa.gov/stp/space-weather/solar-data/solar-indices/total-solar-irradiance/
8. A. L. Morozova, M. I. Pudovkin, and J. V. Black, Geomagn. Aeron. (Engl. Transl.) **39** (2), 40 (1999).
9. V. V. Vityazev, *Wavelet-Analysis of Time Series* (S.-Peterb. Univ., St. Petersburg, 2008) [in Russian].
10. Yu. V. Chernykh, Tr. SPIIRAN **3**, 126 (2003).
11. E. Bruevich, V. Bruevich, and G. Yakuinina, Sun Geosphere **8** (2), 83 (2014).
12. E. A. Bruevich and E. V. Kononovich, Moscow Univ. Phys. Bull. **66**, 72 (2011). doi: 10.3103/S0027134911010073
13. E. Bruevich and I. Alekseev, Astropysics **50**, 187 (2007).
14. I. M. Livshits and V. N. Obridko, Astron. Rep. **50**, 926 (2006).
15. G. S. Ivanov-Kholodnyi, E. I. Mogilevskii, and V. E. Chertoprud, Geomagn. Aeron. (Engl. Transl.) **43**, 151 (2003).
16. Yu. A. Nogovitsyn, Geomagn. Aeron. (Engl. Transl.) **41**, 680 (2001).
17. Yu. A. Nagovitsyn, Astrophys. Bull. **63**, 43 (2008).

Translated by E. Petrova